Journal of Organometallic Chemistry 696 (2011) 4039–4045

Contents lists available at ScienceDirect

Journal of Organometallic Chemistry

journal homepage: www.elsevier.com/locate/jorganchem

Fluorogenic *N*,*O*-chelates built on a C_2-symmetric aryleneethynylene platform: Spectroscopic and structural consequences of conformational preorganization and ligand denticity

Byung Gyu Park, Maren Pink, Dongwhan Lee*

Department of Chemistry, Indiana University, 800 East Kirkwood Avenue, Bloomington, IN 47405, USA

ARTICLE INFO

Article history:
Received 29 April 2011
Accepted 6 July 2011

Dedicated to Professor Kenneth G. Caulton on the occasion of his 70th birthday.

Keywords:
Aryleneethynylene
Conformational preorganization
Multidentate ligand
Fluorescence sensing

ABSTRACT

Using π-extended aryleneethynylene as a rigid structural skeleton, a C_2-symmetric bis(picolinate) ligand was prepared. Binding of zinc(II) or cadmium(II) ion to this formally tetradentate N_2O_2-chelate resulted in significant red-shifts and enhancement in emission. The metal–ligand interaction responsible for such structural change was investigated by isolation and characterization of a tetrazinc(II) complex, in which the picolinate group functions not only as terminal bidentate but also as bridging with its μ-1,3 carboxylate unit.

1. Introduction

A phenylene(ethynylene)-based C_2-symmetric scaffold can bring multiple functional groups into close proximity. As illustrated in Scheme 1, torsional motions about the bis(ethynylphenyl) “axle” of a prototypical structure **I** define finite trajectories to be taken by the two “flap” components. If functionalized with appropriate donor groups, these mobile components converge to support a tight coordination sphere around the metal center in the “folded” conformer. Conceptually related switching motions of “molecular hinges” **II**–**V**, shown in Scheme 1, are driven by host–guest interaction [1], π–π stacking [2,3], or reversible formation of Schiff bases with exogenously added amine substrates [4]. The low-energy barrier of bond rotations around rigid aryleneethynylene-base π-axis has also been exploited in a large number of molecular devices and switches [5–17].

We have recently shown that metalation of one such molecule **L1** (Fig. 1) not only rigidifies its π-conjugated molecular backbone but also profoundly impacts its inherent emission properties [18]. For selected d^{10} metal ions, such as Zn(II), Cd(II), and Hg(II), binding resulted in a ratiometric fluorescence response with systematic buildup of red-shifted bands and correlated decay of the ligand emission.

With the proof-of-concept established, we decided to explore the effects of structural variations made for the bidentate donor motif. Specifically, by replacing the *N*,*N*-bidentate 2,2′-bipyridyl fragment in the parent system **L1** with the *N*,*O*-bidentate picolinate in the new ligand **L2** (Fig. 1), we wished to investigate the effects of harder donor atoms and wider range of bite angles supported by the carboxylate (in **L2**) compared with the pyridyl (in **L1**) analogue. The experimental observables of primary interest are (i) mode of binding, (ii) changes in optical properties, and (iii) selectivities in metal recognition by this new fluorogenic ligand. The design, synthesis, and metal-binding properties of the phenylene(ethynylene)-based ligand **L2** constitute the main topics of this paper.

2. Results and discussions

2.1. Ligand design and synthesis

The C_2-symmetry and built-in modularity of the target molecule simplified our synthetic design as outlined in Scheme 2. A high-yielding C–C coupling under standard Sonogashira–Hagihara reaction conditions converted the known compound **1** to **2**, which was deprotected and subjected to another round of cross-coupling with **4**. The choice of the particular substrate **4** takes into account the higher reactivity of the iodo-substituted carbon, compared with the triflate-substituted carbon, in cross-coupling. Indeed, the

---

* Corresponding author. Tel.: +1 812 855 9364; fax: +1 812 855 8300.
E-mail address: dongwhan@indiana.edu (D. Lee).

0022-328X/$ – see front matter © 2011 Elsevier B.V. All rights reserved.
doi:10.1016/j.jorganchem.2011.07.007

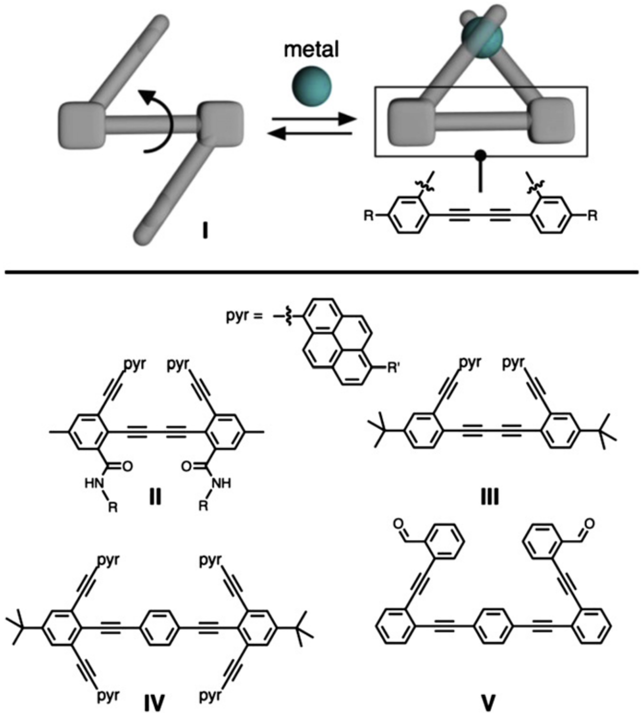

Scheme 1. Metal binding-induced conformational switching of a bis(phenylethynylene)-based C_2-symmetric scaffold **I**. Molecular hinges **II**–**V** also display similar folding–unfolding motions [1–4].

reaction proceeded in high yield (86%) at room temperature to the desired product **5**. At an elevated temperature, **5** was coupled with silyl-protected acetylene to establish the *ortho*-diethynyl substitution pattern in **6**. Desilylation under standard conditions furnished the “half-ligand” molecule **7**, which was subjected to oxidative homocoupling to assemble the C_2-symmetric **8**. The ester groups in **8** were hydrolyzed under basic conditions to complete the synthesis of **9** in overall seven steps. Deprotonation of **9** under metalation conditions furnishes **L2** (*vide infra*).

2.2. Structural and optical properties of the ligand

In $CDCl_3$, **9** displays a highly simplified ^1H NMR pattern, which is consistent with the molecular C_2-symmetry. Notably, the pyridyl proton resonances of **9** at 8.00–8.91 ppm remain largely unchanged relative to those of the “half-ligand” model **7** at 7.97–8.88 ppm, suggesting that the molecule adopts its “unfolded” conformation (Scheme 1) with no significant intramolecular π–π stacking between pyridyl groups. As shown in Fig. 2, both the UV–vis and fluorescence spectra of **L2** are similar to those of **L1**, which corroborates the notion that their low-energy electronic transitions arise from extended π-conjugation along the common bis(phenylethynylene) backbone [18].

2.3. Metal-binding studies

Our previous work has established that the bis(bipy) ligand **L1** forms a stable 1:1 complex with zinc(II) in solution with significant red-shift ($\Delta\lambda_{max}$ = 105 nm) and enhancement in fluorescence emission [18]. Both **L1** and **L2** share an identical phenylene(ethynylene) backbone, and the five-membered chelate ring supported by the *N*,*N*-bidentate donor in **L1** is essentially superimposable with that of *N*,*O*-bidentate in **L2**. As such, simple structural modeling did not suggest any obvious structural deviations that would result from replacing **L1** with **L2** for an octahedral metal complex.

By treating **9** with Et_3N (3 equiv), the ligand of **L2** was generated in situ, which was subsequently titrated with Zn^{2+} in MeCN. This process was followed by both UV–vis and fluorescence spectroscopy. As shown in Fig. 3a, metalation of **L2** resulted in a gradual decrease in the intensity of the absorption peak at $\lambda_{max} = 300$ nm. The changes in emission under similar conditions, however, revealed a rather complicated pattern. As shown in Fig. 3b, addition of up to 1 equiv of Zn(II) resulted in an enhancement in the emission intensity at $\lambda_{max,em} = 390$ and 415 nm, but no shift in the emission wavelength. A further loading of metal ions, however, elicited a decrease in this ligand fluorescence with appearance of a new broad lower-energy emission at $\lambda_{max,em} = 455$ nm (Fig. 3b).

With the fluorescence response of **L2** toward Zn(II) demonstrated, we proceeded to investigate the scope of this chemistry across an expanded set of metal ions. As shown in Fig. 4a, addition of Hg(II), Pb(II), Ag(I), Fe(II), Cu(I), Mn(II), Co(II), Ni(II), or Cu(II) to **L2** in MeCN resulted in a complete quenching of the ligand fluorescence. Under similar conditions, however, both Zn(II) and Cd(II) elicited an enhancement and significant red-shift ($\Delta\lambda = 65$ nm) in the emission. A quantitative analysis of this process was aided by comparing changes in the normalized emission intensity at $\lambda = 500$ nm prior to and after metalation (Fig. 4b). As is evident from this plot, **L2** responds selectively only to Zn(II) and Cd(II), whereas their congener Hg(II) and other metal ions simply quench the emission.

By participating in excited-state energy transfer (EET) or electron-transfer (ET) pathways, many open–shell transition metal ions quench ligand fluorescence [19–24]. Certain closed-shell metal ions, however, do not promote such non-radiative decay, and even give rise to enhanced emission through the inversion of the $n\pi^*$–$\pi\pi^*$ ligand excited-states upon metal-binding [25]. The fluorescence response of **L1** and **L2** toward various metal ions might thus be explained within this general paradigm of

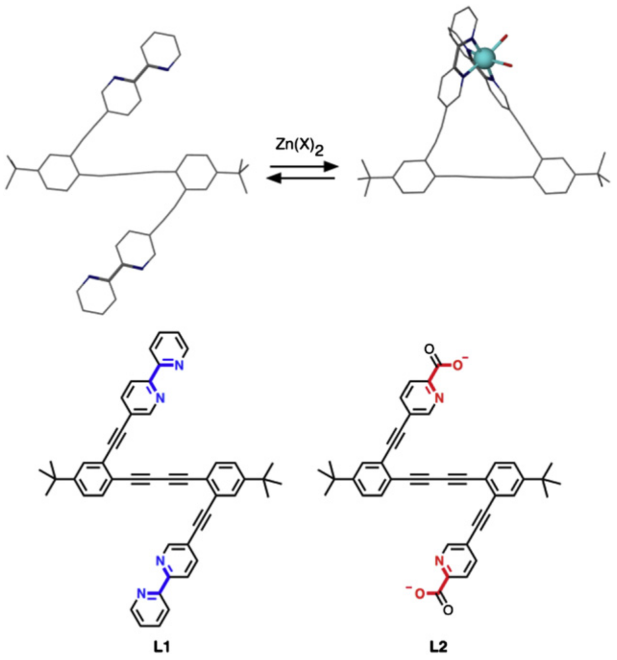

Fig. 1. Capped-stick representations of the X-ray structures of free ligand **L1** and its Zn(II) complex [Zn(**L1**)X_2] (X = OTf$^-$), where only the oxygen donor atoms are shown for the two terminally bound triflate ligands [18]. Chemical structures of **L1** and **L2** are shown below.

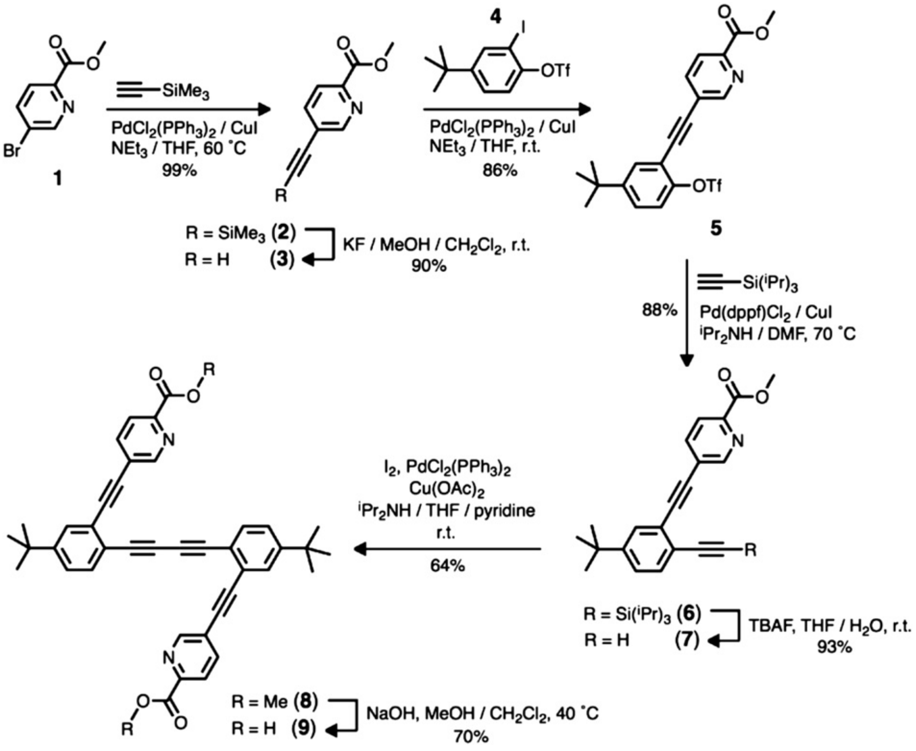

Scheme 2. Synthetic route to **9**.

structure–property relationship, but a notable exception to this empirical trend is Hg(II). While binding of this heavy metal ion to bis(bipy) ligand **L1** results in an enhanced emission, a complete quenching of fluorescence is observed upon metalation of the bis(picolinate) ligand **L2** under similar conditions.

2.4. *Assembly of dinuclear versus tetranuclear clusters*

Upon binding of zinc(II), both **L1** and **L2** show decrease in the ligand emission and development of new red-shifted features. For **L1**, this spectral change entails a genuine ratiometric behavior, in which diminution of the ligand emission at a shorter-wavelength correlates with systematic enhancement in the longer-wavelength emission from the 1:1 complexation event [18]. In contrast, metal-dependent changes in the fluorescence of **L2** progress through multiple stages (Fig. 3b), which could not be explained by invoking a simple 1:1 binding model as in **L1**. Indeed, Job's plot analysis on **L2** (data not shown) revealed no consistent trend to extract information on binding stoichiometry of zinc(II), which implicated the involvement of multiple, metal-containing species, possibly beyond the level of mononuclear complex. Experimental evidence in support of this notion came from X-ray crystallography on the metal complex obtained from the reaction between **L2** and $Zn(ClO_4)_2$ in THF. Vapor diffusion of Et_2O into a THF solution of this material furnished single crystals, which were analyzed by X-ray crystallography.

As shown in Fig. 5, the zinc(II) complex of **L2** has a tetranuclear core, in which each octahedral metal center is coordinated by two nitrogen and four oxygen donor atoms. In this assembly, the ratio between metal and the ligand is still maintained as 1:1, as in **L1** (Fig. 1), but each of the two picolinate fragments in **L2** are coordinated to different metal ions (Fig. 6b). This situation is different from that of the mononuclear Zn(II) complex of **L1**, in which its two bipy fragments converge to a single metal center to function as an overall tetradentate ligand (Fig. 6a). A close inspection of the coordination mode of this intriguing complex revealed that each zinc(II) center is coordinated to three picolinates, each of which is supplied from different **L2** ligands encapsulating the tetranuclear core. Among these, two picolinates function as genuine *N*,*O*-bidentate, whereas one as *O*-monodentate using its carboxylate fragment only (Fig. 6c). The remaining coordination site is occupied by oxygen atoms provided by either ClO_4^- anion or H_2O molecule, which completes the N_2O_4 overall donor combination. Although these ClO_4^-/H_2O ligands are heavily disordered to preclude detailed structural discussion, both the chemical connectivity of the $[Zn_4(\mathbf{L2})_4]^{4+}$ core and the ligand conformation that enables the assembly of this rather unanticipated cluster were unambiguously established.

A question that immediately arises within this context is why **L1** and **L2**, sharing an essentially identical C_2-symmetric skeleton, support such markedly different coordination modes. Unlike the *N*,*N*-bidentate bipy groups in **L1**, the piconlinate groups in **L2** can function as *N*,*O*-bidentate as well as *O*,*O*-bridging ligand (Fig. 6c). Without proper steric protection or conformational restriction

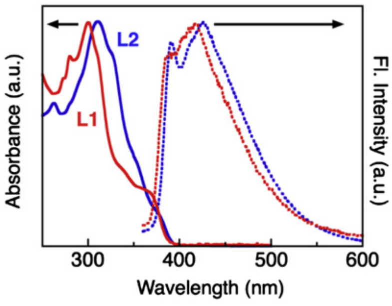

Fig. 2. Normalized UV–vis (solid lines) and emission (broken lines) spectra of **L1** (red) and **L2** (blue) in MeCN. **L2** was generated in situ by treating **9** with Et_3N (3 equiv). (For interpretation of the references to colour in this figure legend, the reader is referred to the web version of this article.)

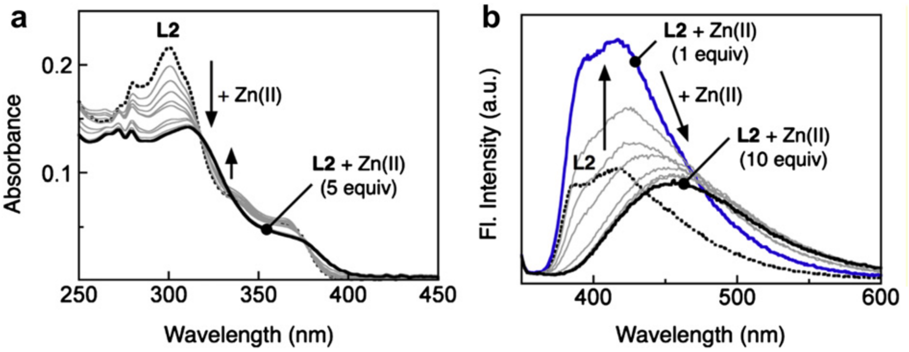

Fig. 3. Changes in the (a) UV–vis spectra of **L2** (5.0 μM) upon addition of Zn(II) (0–25 μM; delivered as triflate salt), and (b) fluorescence spectra of **L2** (0.5 μM) upon addition of Zn(II) (0–5 μM; delivered as triflate salt) in MeCN; $\lambda_{exc} = 310$ nm; $T = 293$ K.

imposed by ancillary ligands [26,27], such structural versatility of picolinate often leads to the formation of an infinite chain/network of coordination polymers [28,29]. For **L2**, however, the cluster formation stops at the tetranuclear stage. As illustrated by the partial X-ray structure (Fig. 6b), one picolinate in each **L2** links two Zn(II) centers using a syn–anti carboxylate ligand. This μ-1,3 bridging pattern makes an essentially 90°-turn at each metal center to enclose a *pseudo*-square marked with four zinc atoms, which have narrowly distributed Zn···Zn interatomic distances of 5.160–5.257 Å (Fig. 5b).

3. Summary

A new bis(picolinate) ligand **L2** was built with a C_2-symmetric π-extended molecular platform, and studied as a fluorescent sensor for selected metal ions. As in its bis(bipy) analogue **L1**, which shares an identical bis(phenylethynylene) backbone, binding of Zn(II) or Cd(II) ions resulted in significant red-shifts in the emission of **L2**. The metal–ligand interaction responsible for such spectral change, however, is more complicated than that of **L1**. Notably, isolation and structural characterization of a tetrazinc(II) complex of **L2** confirmed that the pyridyl-appended carboxylate group functions not only as terminal monodentate but also as μ-1,3 bridging ligand to promote the assembly of a multinuclear cluster. Introduction of harder oxygen donor atoms in **L2** also changed the selectivity: unlike its congeners Zn(II) or Cd(II), Hg(II) ion simply quenched the fluorescence.

4. Experimental section

4.1. General considerations

All reagents were obtained from commercial suppliers and used as received unless otherwise noted. The solvents dichloromethane, diethyl ether, toluene, and THF were saturated with nitrogen and purified by passage through activated Al_2O_3 columns under nitrogen (Innovative Technology SPS 400) prior to use [30]. Triethylamine, diisopropylamine and DMF were saturated with nitrogen and used without further purification. The compound 4-*tert*-butyl-2-iodophenyl trifluoromethanesulfonate (**4**) was prepared according to literature procedures [18]. All air-sensitive manipulations were carried out under nitrogen atmosphere in an M. Braun drybox or by standard Schlenk-line techniques.

4.2. Physical measurements

^{1}H NMR and ^{13}C NMR spectra were recorded on a 400 MHz Varian Inova NMR Spectrometer or a 300 MHz Varian Gemini 2000 NMR spectrometer. Chemical shifts were reported versus tetramethylsilane and referenced to the residual solvent peaks. High-resolution chemical ionization (CI) (using CH_4 as CI reagent) and electrospray ionization (ESI) mass spectra were obtained on a Thermo Electron Corporation MAT 95XP-Trap. MALDI-TOF mass spectra were obtained on Bruker Biflex III MALDI–TOF Mass Spectrometer. FT-IR spectra were recorded on a Nicolet Avatar 360 FT-IR Spectrometer with EZ OMNIC E.S.P. software. UV–vis spectra were recorded on an Agilent 8453 UV–vis spectrophotometer with ChemStation. Fluorescence spectra were recorded on a Photon Technology International QM-4-CW spectrofluorometer with FeliX32 software.

4.3. Crystallization and X-ray structure determination

A THF (1 mL) solution of **9** (60 mg, 0.10 mmol) was treated with a solution of $Zn(ClO_4)_2 \cdot 6H_2O$ (37 mg, 0.10 mmol) in THF (5 mL). The mixture was stirred for 1 h at r.t. under nitrogen. Volatile fractions were removed under reduced pressure to obtain a yellow solid. Yellow plates suitable for X-ray crystallography were grown by

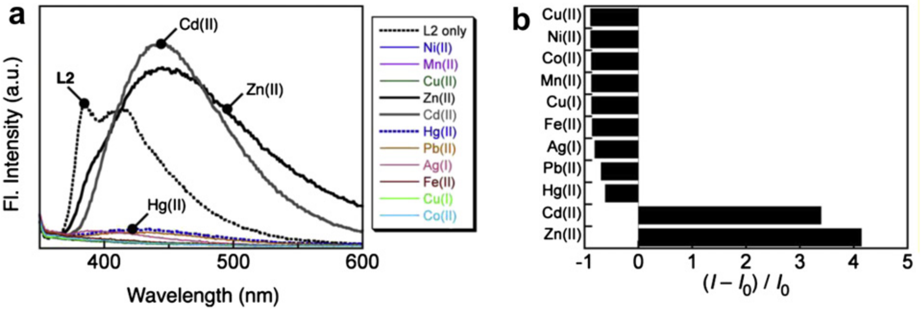

Fig. 4. (a) Changes in the fluorescence spectra of **L2** (0.5 μM) upon addition of various metal ions (5.0 μM) in MeCN. In (b), the fluorescence response was quantified by the ratio $(I-I_0)/I_0$, where I_0 and I denote the emission intensity at $\lambda = 500$ nm prior to and after addition of the metal ion, respectively. $\lambda_{exc} = 310$ nm; $T = 293$ K.

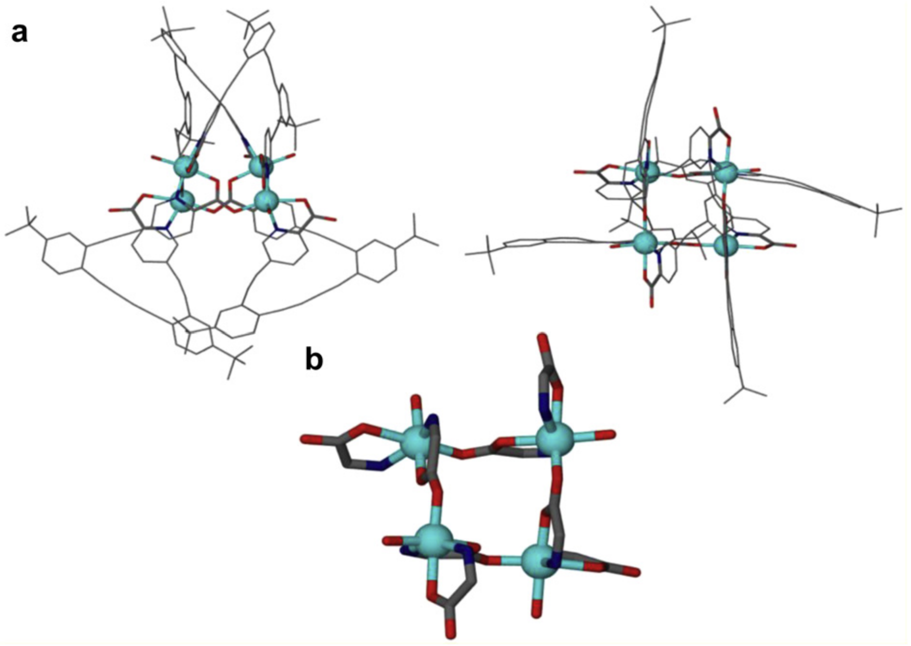

Fig. 5. (a) Capped-stick representation of the $[Zn_4(\mathbf{L2})_4(X)_4]^{n+}$ core generated using X-ray coordinates and viewed from two different perspectives. (b) A close-up view of the tetrazinc(II) core, in which the picolinate ligands are abbreviated as the N–C–C(=O)–O skeleton. The terminal ligand X is either ClO_4^- or H_2O, for which only the oxygen donor atom is shown for clarity.

vapor diffusion of Et_2O into a THF solution of this material. A singe-crystal was placed onto the tip of a 0.1 mm diameter glass capillary and mounted on a Bruker APEX II Kappa Duo diffractometer equipped with an APEX II detector at 120(2) K. The data collection was carried out using Mo Kα radiation (graphite monochromator) with a frame time of 50 s. Details of crystal data collection and analysis are given in the Supplementary material. The final full matrix least squares refinement converged to $R1 = 0.1083$ and $wR2 = 0.3263$ (F^2, all data). Restraints and constraints were applied in the refinement. The remaining electron density is located in voids in the structure and no chemically reasonable pattern could be refined for residual peaks. Connectivity and overall geometry of the tetrazinc(II) complex were unequivocally established.

4.4. Synthesis of methyl 5-((trimethylsilyl)ethynyl)picolinate *2*

A 100-mL round bottom flask was loaded with methyl 5-bromopicolinate (1.00 g, 4.63 mmol), $PdCl_2(PPh_3)_2$ (66 mg, 0.093 mmol), and CuI (27 mg, 0.14 mmol) under nitrogen atmosphere. A mixture of NEt_3/THF (30 mL, 1:1, v/v) was added under nitrogen, followed by ethynyltrimethylsilane (2.0 mL, 14 mmol). The solution was stirred at 60 °C for 18 h under nitrogen. The crude reaction mixture was filtered through a pack of Celite, and the filtrate concentrated under reduced pressure. The residual brown oil was purified by flash column chromatography on SiO_2 (hexanes:EtOAc = 9:1, v/v) to afford **2** as a brown solid (1.07 g, 99%). ^1H NMR (400 MHz, $CDCl_3$, 298 K): δ 8.76 (dd, $J = 2.0, 0.7$ Hz, 1H), 8.07 (dd, $J = 8.1, 0.7$ Hz, 1H), 7.87 (dd, $J = 8.1, 2.0$ Hz, 1H), 4.00 (s, 3H), 0.27 (s, 9H); ^{13}C NMR (100 MHz, $CDCl_3$, 298 K): δ 165.3, 152.5, 146.3, 139.9, 124.5, 123.9, 102.1, 100.7, 53.2, −0.2. FT-IR (thin film on NaCl, cm^{-1}): 2957, 1716, 1444, 1368, 1313, 1246, 1225, 1194, 1134, 1018, 868, 843, 794, 760, 701. HRMS (CI) calcd for $C_{12}H_{16}NO_2Si$ $[M + H]^+$ 234.0945, found 234.0949.

4.5. Synthesis of methyl 5-ethynylpicolinate *3*

To a stirred solution of **2** (1.08 g, 4.63 mmol) in CH_3OH/CH_2Cl_2 (30 mL, 1:1, v/v) was added KF (1.31 g, 13.9 mmol) as a solid. After complete consumption of the starting material (2 h), the crude reaction mixture was filtered and concentrated under reduced pressure. The residual brown solid was purified by flash column chromatography on SiO_2 (hexanes:EtOAc = 4:1, v/v) to afford **3** as a yellow solid (0.67 g, 90%). ^1H NMR (300 MHz, $CDCl_3$, 298 K): δ 8.79 (d, $J = 2.0$ Hz, 1H), 8.08 (d, $J = 8.0$ Hz, 1H), 7.90 (dd, $J = 8.0, 2.0$ Hz, 1H), 4.00 (s, 3H), 3.37 (s, 1H); ^{13}C NMR (75 MHz, $CDCl_3$, 298 K): δ 165.2, 152.7, 146.9, 140.2, 124.5, 122.8, 83.6, 79.8, 53.2. FT-IR (thin film on NaCl, cm^{-1}): 3444, 3254, 3097, 3066, 3015, 1726, 1581, 1555, 1455, 1362, 1311, 1275, 1241, 1206, 1120, 1018, 878, 793, 701, 679. HRMS (CI) calcd for $C_9H_8NO_2$ $[M + H]^+$ 162.0550, found 162.0543.

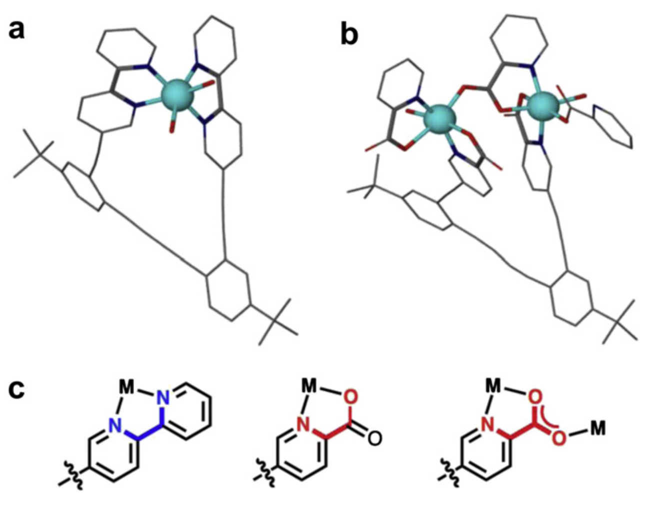

Fig. 6. Capped-stick representations of (a) $[Zn(\mathbf{L1})(OTf)_2]$ and (b) dinuclear substructure of $[Zn_4(\mathbf{L2})_4(X)_4]^{n+}$ (X = H_2O or ClO_4^-; shown by oxygen donor atom only) generated using X-ray coordinates. Different coordination modes of 2,2′-bipy (in **L1**) and picolinate (in **L2**) ligands are compared in (c).

4.6. Synthesis of methyl 5-((5-tert-butyl-2-(trifluoromethylsulfonyloxy)phenyl)ethynyl)picolinate ***5***

A mixture of **4** (1.70 g, 4.16 mmol), **3** (0.670 g, 4.16 mmol), $PdCl_2(PPh_3)_2$ (60 mg, 0.083 mmol), and CuI (24 mg, 0.012 mmol) in NEt_3/THF (20 mL, 1:1, v/v) was stirred at room temperature under nitrogen atmosphere for 18 h. The crude reaction mixture was filtered through a pack of Celite, and the filtrate concentrated under reduced pressure. The residual brown solid was purified by flash column chromatography on SiO_2 (hexanes:EtOAc = 4:1, v/v) to afford **5** as a yellow solid (1.57 g, 86%). ^1H NMR (400 MHz, $CDCl_3$, 298 K): δ 8.91 (s, 1H), 8.15 (d, $J = 8.0$ Hz, 1H), 8.02 (dd, $J = 8.0, 2.0$ Hz, 1H), 7.67 (d, $J = 2.4$ Hz, 1H), 7.48 (dd, $J = 8.8, 2.4$ Hz, 1H), 7.24 (d, $J = 8.8$ Hz, 1H), 4.03 (s, 3H), 1.35 (s, 9H); ^{13}C NMR (100 MHz, $CDCl_3$, 298 K): δ 165.3, 152.2, 152.0, 147.8, 146.8, 139.7, 131.0, 128.4, 124.7, 123.2, 121.4, 116.6, 91.5, 89.2, 53.2, 35.0, 31.2. FT-IR (thin film on NaCl, cm^{-1}): 2962, 1746, 1725, 1584, 1552, 1493, 1425, 1368, 1310, 1278, 1213, 1140, 1119, 1077, 1023, 927, 875, 638, 617. HRMS (CI) calcd for $C_{20}H_{19}F_3NO_5S$ $[M + H]^+$ 442.0931, found 442.0938.

4.7. Synthesis of methyl 5-((5-tert-butyl-2-((triisopropylsilyl)ethynyl)phenyl)ethynyl)picolinate ***6***

A 100-mL round bottom flask was loaded with **5** (1.57 g, 3.65 mmol), $PdCl_2(dppf)\cdot CH_2Cl_2$ (90 mg, 0.11 mmol), and CuI (40 mg, 0.21 mmol) under nitrogen atmosphere. A mixture of DMF/$^iPr_2NH$ (30 mL, 1:1, v/v) was added under nitrogen, followed by ethynyltriisopropylsilane (1.60 mL, 7.11 mmol). The solution was stirred at 70 °C for 48 h under nitrogen, and filtered through a pack of Celite. The filtrate was diluted with Et_2O (100 mL), and washed with water (3 × 100 mL) and brine (100 mL). The organic layer was dried over anhydrous $MgSO_4$, filtered, and concentrated under reduced pressure. The residual material was purified by flash column chromatography on SiO_2 (hexanes:EtOAc = 10:1, v/v) to afford **6** as a brown viscous oil (1.49 g, 88%). ^1H NMR (400 MHz, $CDCl_3$, 298 K): δ 8.85 (d, $J = 1.2$ Hz, 1H), 8.12 (d, $J = 8.0$ Hz, 1H), 7.95 (dd, $J = 8.0, 2.0$ Hz, 1H), 7.57 (d, $J = 1.6$ Hz, 1H), 7.47 (d, $J = 8.4$ Hz, 1H), 7.35 (dd, $J = 8.0, 2.0$ Hz, 1H), 4.03 (s, 3H), 1.32 (s, 9H), 1.10 (s, 21H); ^{13}C NMR (100 MHz, $CDCl_3$, 298 K): δ 165.3, 152.2, 151.8, 146.2, 139.6, 132.8, 129.4, 126.5, 124.5, 124.3, 124.2, 123.4, 105.2, 95.2, 95.1, 88.2, 53.2, 35.0, 31.2, 18.8, 11.4. FT-IR (thin film on NaCl, cm^{-1}): 2956, 2865, 1748, 1725, 1491, 1462, 1436, 1308, 1234, 1162, 1131, 1072, 1022, 883, 828, 672. HRMS (CI) calcd for $C_{30}H_{40}NO_2Si$ $[M + H]^+$ 474.2823, found 474.2804.

4.8. Synthesis of methyl 5-((5-tert-butyl-2-ethynylphenyl)ethynyl)picolinate ***7***

To a stirred solution of **6** (1.49 g, 3.14 mmol) in THF/H_2O (30 mL, 10:1, v/v) was added TBAF (9.0 mL, 1.0 M solution in THF) in a dropwise fashion. The mixture was stirred for 3 h, diluted with water (50 mL), and extracted with CH_2Cl_2 (3 × 50 mL). The combined organic extracts were washed with water (3 × 30 mL), dried over anhydrous $MgSO_4$, filtered, and concentrated under reduced pressure. The residual material was purified by flash column chromatography on SiO_2 (hexanes:EtOAc = 4:1 to 2:1, v/v) to afford **7** as a brown solid (0.93 g, 93%). ^1H NMR (400 MHz, $CDCl_3$, 298 K): δ 8.88 (d, $J = 2.0$ Hz, 1H), 8.12 (d, $J = 8.0$ Hz, 1H), 7.97 (dd, $J = 8.0, 2.0$ Hz, 1H), 7.58 (d, $J = 1.6$ Hz, 1H), 7.49 (d, $J = 8.4$ Hz, 1H), 7.37 (dd, $J = 8.0, 2.0$ Hz, 1H), 4.02 (s, 3H), 3.33 (s, 1H), 1.33 (s, 9H); ^{13}C NMR (100 MHz, $CDCl_3$, 298 K): δ 165.4, 152.3, 152.2, 146.3, 139.5, 132.7, 129.2, 126.6, 124.7, 124.6, 124.1, 122.3, 94.8, 88.7, 82.0, 81.0, 53.1, 35.0, 31.1. FT-IR (thin film on NaCl, cm^{-1}): 3285, 2959, 2906, 1743, 1723, 1584, 1435, 1366, 1308, 1276, 1259, 1234, 1194, 1163, 1131, 1022, 836, 702. HRMS (CI) calcd for $C_{21}H_{20}NO_2$ $[M + H]^+$ 318.1489, found 318.1485.

4.9. Synthesis of dimethyl 5,5′-(6,6′-(buta-1,3-diyne-1,4-diyl)bis(3-tert-butyl-6,1-phenylene)bis(ethyne-2,1-diyl))dipicolinate ***8***

A 100-mL round bottom flask was loaded with **7** (0.77 g, 3.2 mmol), $PdCl_2(PPh_3)_2$ (44 mg, 0.063 mmol), and $Cu(OAc)_2$ (29 mg, 0.16 mmol). A mixture of THF/$^iPr_2NH$ (10 mL, 1:1, v/v) and pyridine (2 mL) was added, followed by I_2 (0.40 g, 1.6 mmol). After stirring at room temperature for 2 h under air, the reaction was completed as judged by TLC. The crude reaction mixture was filtered through a pack of Celite and the isolated solid material was extracted with $CHCl_3$ (3 × 150 mL). The organic layer was washed with water (3 × 100 mL), dried over anhydrous $MgSO_4$, filtered, and concentrated under reduced pressure. The crude solid was washed with Et_2O (100 mL) and concentrated under reduced pressure to afford **8** as a pale yellow solid (0.64 g, 64%). ^1H NMR (400 MHz, $CDCl_3$, 298 K): δ 8.87 (d, $J = 1.6$ Hz, 2H), 8.03 (d, $J = 8.0$ Hz, 2H), 7.98 (dd, $J = 8.0, 2.0$ Hz, 2H), 7.61 (d, $J = 2.0$ Hz, 2H), 7.54 (d, $J = 8.4$ Hz, 2H), 7.42 (dd, $J = 8.4, 2.0$ Hz, 2H), 4.00 (s, 6H), 1.36 (s, 18H); ^{13}C NMR (100 MHz, $CDCl_3$, 298 K): δ 165.4, 153.0, 152.2, 146.2, 139.7, 132.9, 129.3, 126.8, 125.6, 124.6, 124.0, 122.1, 94.7, 89.5, 81.3, 77.7, 53.1, 35.2, 31.1. FT-IR (thin film on NaCl, cm^{-1}): 2958, 1745, 1723, 1586, 1436, 1366, 1308, 1276, 1259, 1234, 1194, 1163, 1131, 1023, 832, 750, 701. HRMS (ESI) calcd for $C_{42}H_{37}N_2O_4$ $[M + H]^+$ 633.2753, found 633.2721.

4.10. Synthesis of 5,5′-(6,6′-(buta-1,3-diyne-1,4-diyl)bis(3-tert-butyl-6,1-phenylene)bis(ethyne-2,1-diyl))dipicolinic acid ***9***

To a stirred solution of **8** (0.22 g, 0.34 mmol) in CH_2Cl_2/CH_3OH (30 mL, 3:2, v/v) was added a solution of NaOH (41 mg, 1.0 mmol) in CH_3OH (4 mL). After stirring at 40 °C for 3 h, the reaction was completed as judged by TLC. The reaction mixture was diluted with water (50 mL), and an aqueous solution of HCl (1 M) was added to adjust the pH to 4. The mixture was diluted with EtOAc (150 mL). The organic layer was separated, washed with water (3 × 30 mL), dried over anhyd $MgSO_4$, filtered, and concentrated under reduced pressure. The residual solid material was washed with Et_2O (50 mL), and dried in vacuo to afford **9** as a brown solid (144 mg, 70%). ^1H NMR (400 MHz, $CDCl_3$, 298 K): δ 8.91 (s, 2H), 8.06 (d, $J = 8.0$ Hz, 2H), 8.00 (dd, $J = 8.0, 1.6$ Hz, 2H), 7.68 (s, 2H), 7.54 (d, $J = 8.4$ Hz, 2H), 7.45 (dd, $J = 8.4, 2.0$ Hz, 2H), 1.40 (s, 18H); ^{13}C NMR (100 MHz, $CDCl_3$, 298 K): δ 164.9, 153.3, 149.9, 146.4, 141.1, 131.9, 129.3, 126.8, 126.3, 124.8, 124.2, 122.4, 95.2, 89.3, 81.5, 78.0, 35.2, 31.1. FT-IR (thin film on NaCl, cm^{-1}): 3422, 1697, 1583, 1554, 1413, 1362, 1307, 1260, 1232, 1166, 1146, 1118, 1030, 833, 796, 729, 695. HRMS (CI) calcd for $C_{40}H_{33}N_2O_4$ $[M + H]^+$ 605.2435, found 605.2441.

Acknowledgment

This work was supported by the National Science Foundation (CHE 0547251) and Grant No. 00035484 from the SMBA of Korea.

Appendix A. Supplementary material

CCDC 822961 contains the supplementary crystallographic data for this paper. This data can be obtained free of charge from The Cambridge Crystallographic Data Center via www.ccdc.cam.ac.uk/data-request/cif.

References

[1] S. Yagi, H. Kitayama, T. Takagishi, J. Chem. Soc. Perkin Trans. 1 (2000) 925–932.
[2] S. Sankararaman, G. Venkataramana, B. Varghese, J. Org. Chem. 73 (2008) 2404–2407.
[3] R. Nandy, M. Subramoni, B. Varghese, S. Sankararaman, J. Org. Chem. 72 (2007) 938–944.
[4] D. Iwaniuk, C. Wolf, J. Am. Chem. Soc. 133 (2011) 2414–2417.
[5] P.J. Stang, F. Diederich (Eds.), Modern Acetylene Chemistry, VCH, Weinheim, Germany, 1995.
[6] F. Diederich, P.J. Stang, R.R. Tykwinski (Eds.), Acetylene Chemistry: Chemistry, Biology, and Material Science, Wiley–VCH, Weinheim, Germany, 2005.
[7] V. Balzani, M. Venturi, A. Credi, Molecular Devices and Machines: A Journey into the Nanoworld. Wiley–VCH, Weinheim, 2003.
[8] G.S. Kottas, L.I. Clarke, D. Horinek, J. Michl, Chem. Rev. 105 (2005) 1281–1376.
[9] T.F. Magnera, J. Michl, Top. Curr. Chem. 262 (2005) 63–97.
[10] S. Toyota, Chem. Rev. 110 (2010) 5398–5424.
[11] T.C. Bedard, J.S. Moore, J. Am. Chem. Soc. 117 (1995) 10662–10671.
[12] J.S. Moore, Acc. Chem. Res. 30 (1997) 402–413.
[13] S.D. Karlen, M.A. Garcia-Garibay, Top. Curr. Chem. 262 (2005) 179–227.
[14] T.-A.V. Khuong, J.E. Nuñez, C.E. Godinez, M.A. Garcia-Garibay, Acc. Chem. Res. 39 (2006) 413–422.
[15] P.D. Jarowski, K.N. Houk, M.A. Garcia-Garibay, J. Am, Chem. Soc. 129 (2007) 3110–3117.
[16] Y. Shirai, J.-F. Morin, T. Sasaki, J.M. Guerrero, J.M. Tour, Chem. Soc. Rev. 35 (2006) 1043–1055.
[17] G. Vives, J.M. Tour, Acc. Chem. Res. 42 (2009) 473–487.
[18] X. Jiang, B.G. Park, J.A. Riddle, B.J. Zhang, M. Pink, D. Lee, Chem. Commun. (2008) 6028–6030.
[19] J.C. Dederen, M. Van der Auweraer, F.C. De Schryver, J. Phys. Chem. 85 (1981) 1198–1202.
[20] L. Fabbrizzi, A. Poggi, Chem. Soc. Rev. 24 (1995) 197–202.
[21] R. Bergonzi, L. Fabbrizzi, M. Licchelli, C. Mangano, Coord. Chem. Rev. 170 (1998) 31–46.
[22] V. Amendola, L. Fabbrizzi, M. Licchelli, C. Mangano, P. Pallavicini, L. Parodi, A. Poggi, Coord. Chem. Rev. 190–192 (1999) 649–669.
[23] J.R. Lakowicz, Principles of Fluorescence Spectroscopy, third ed. Springer, New York, 2006.
[24] N. Rupcich, W. Chiuman, R. Nutiu, S. Mei, K.K. Flora, Y. Li, J.D. Brennan, J. Am. Chem. Soc. 128 (2006) 780–790.
[25] A.P. de Silva, H.Q.N. Gunaratne, T. Gunnlaugsson, A.J.M. Huxley, C.P. McCoy, J.T. Rademacher, T.E. Rice, Chem. Rev. 97 (1997) 1515–1566.
[26] N.V. Kaminskaia, B. Spingler, S.J. Lippard, J. Am. Chem. Soc. 123 (2001) 6555–6563.
[27] Z. Vargová, J. Kotek, J. Rudovský, J. Plutnar, R. Gyepes, P. Hermann, K. Györyová, I. Lukeš, Eur. J. Inorg. Chem. 2007 (2007) 3974–3987.
[28] Y.-T. Wang, H.-H. Fan, H.-Z. Wang, X.-M. Chen, Inorg. Chem. 44 (2005) 4148–4150.
[29] C. Papatriantafyllopoulou, C.P. Raptopoulou, A. Terzis, J.F. Janssens, E. Manessi-Zoupa, S.P. Perlepes, J.C. Plakatouras, Polyhedron 26 (2007) 4053–4064.
[30] A.B. Pangborn, M.A. Giardello, R.H. Grubbs, R.K. Rosen, F.J. Timmers, Organometallics 15 (1996) 1518–1520.